Double Proton Transfer Reaction of 7-Azaindole Dimer and Complexes Studied by Time-Resolved Thermal Lensing Technique

Tadashi Suzuki, Ushio Okuyama, and Teijiro Ichimura*

Department of Chemistry, Tokyo Institute of Technology, 2-12-1 Ohokayama, Meguro-ku, Tokyo 152, Japan

Received: June 3, 1997[⊗]

Time-resolved thermal lensing (TRTL) technique was applied to the determination of enthalpy change in double proton transfer reaction of 7-azaindole (AI) dimer and its complexes with acetic acid (AcOH) and methanol in solution. Excited AI dimer/complexes emit violet fluorescence or undergo rapid double proton transfer (DPT) reaction to form excited tautomers, which emit green fluorescence. The emission quantum yields were successfully determined with a calorimetric standard of pyridazine to be 0.00_6 (AI dimer), 0.16 (AI dimeric tautomer), 0.00_2 (AI−AcOH complex), 0.11 (AI−AcOH tautomer), and 0.08 (AI−methanol complex). By analyzing the time evolution of TRTL signals of AI dimer, the lifetime of the tautomer in the ground state was determined to be 19 μs, which well agreed with the values obtained with flash photolysis and stepwise two-color laser-induced fluorescence experiments. The enthalpy change of the tautomer to the AI dimer in the ground state was obtained to be surprisingly low, 340 cm^{-1}. The TRTL results under high photon density excitation show that AI dimer easily absorbs second photon to dissociate into two monomeric tautomers followed by the recombination in *ca*. 2 ms.

Introduction

The excited state dynamics of 7-azaindole (AI) dimer and its complexes have been extensively studied in the condensed phase[1−14] and in supersonic jet expansion[15−18] because of photochemical and photobiological interest. The excited state double proton transfer (DPT) reaction of AI dimer, regarded as a model of hydrogen-bonded base pair in the double-stranded DNA helix, has been proposed to be a mechanism for the initial step in photomutagenesis of DNA.[1−3] Figure 1 shows the schematic energy diagram of AI dimer/complexes and their tautomers. After excitation, violet and green emissions were observed and ascribed to the excited dimer and the tautomer generated by the excited state double proton transfer reaction, respectively.

Pico- and femtosecond studies have been carried out to elucidate the reaction mechanism for the AI dimer.[4,5,18] The rise time of the tautomer fluorescence was reported to vary from less than 5 ps at room temperature to *ca*. 1 ns at 77 K.[4] This temperature dependence reveals a thermal activation barrier for the excited state DPT reaction. Share *et al*. reported with the femtosecond study that the excited state DPT reaction proceeds at 1.4 ps and the tautomer in the ground state is formed within a laser pulse duration, suggesting that the reaction should occur through two parallel paths.[5] Fuke *et al*. concluded that the excited state DPT reaction of AI dimer has no energy barrier since it occurs even from the zero vibrational level of the dimer S_1 state with a supersonic jet spectroscopy.[15,16] Recently, femtosecond mass spectroscopy was applied to clarify the reaction mechanism in the isolated system; the protons on each AI molecule move sequentially to the other through an intermediate state.[18] *Ab initio* calculation postulated that the intermediate state is slightly stable than transition states.[19]

In contrast, the excited state DPT reaction of hydrogen-bonded complexes with water, alcohols, and acids, which are used as a solvent, was relatively slower.[6−11,14] It is pointed out that solvation affects the reaction dynamics; that is, cyclic 1:1 AI/ROH complex undergoes the tautomerization reaction, but blocked 1:2 complex does not.

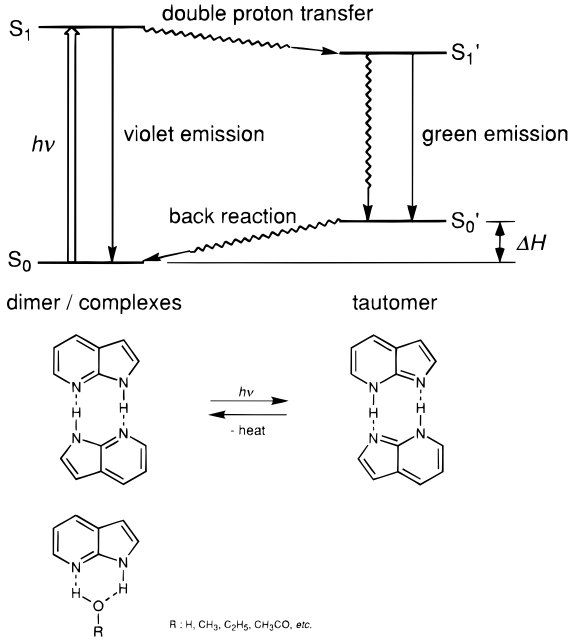

Figure 1. Reaction scheme of AI dimer/complexes. Excited dimer/complexes emit violet fluorescence or undergoes rapid DPT reaction to produce excited tautomer, which emits green fluorescence. Finally, back DPT reaction occurs from the tautomer in the ground state to the AI dimer. ΔH shows the enthalpy difference for the back DPT reaction.

On the other hand, an energy barrier for the black DPT reaction of AI dimer in 3-methylpentane has been reported with transient absorption and two-step laser excitation techniques.[12,13] The barrier was estimated to be 1.4 kcal/mol from an Arrhenius plot in the narrow temperature range (240−280 K) because the plot was curved due to quantum mechanical tunneling. The enthalpy difference between the tautomer and the dimer in the ground states was speculated with *ab initio* calculations to be 93 and 102 kJ/mol.[14,19] However, it has been difficult to

* To whom correspondence should be addressed. E-mail: tichimur@chem.titech.ac.jp.

⊗ Abstract published in *Advance ACS Abstracts,* September 1, 1997.

S1089-5639(97)01790-8 CCC: $14.00

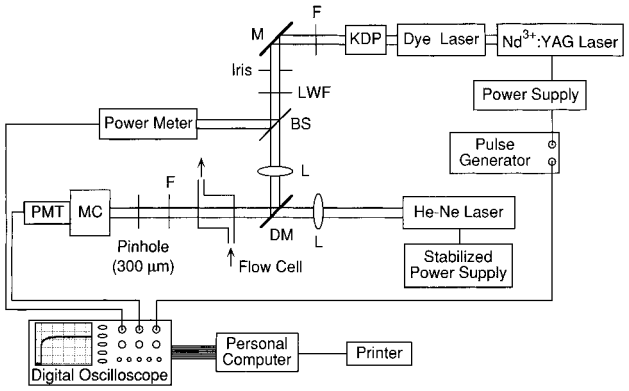

Figure 2. Experimental setup for TRTL measurements: F, filter; M, mirror; L, lens; BS, beam splitter; LWF, gradient linear wedge filter; DM, dichroic mirror; MC, monochromator; PMT, photomultiplier tube.

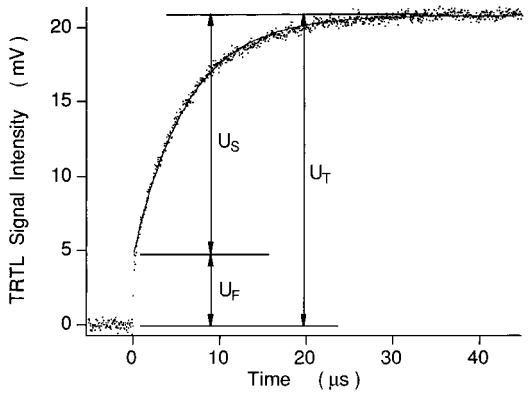

Figure 3. Typical TRTL time profile of benzophenone in benzene with 320 nm excitation, composed of fast and slow rising parts. The fast component corresponds to heat released with the production of triplet state from initially excited singlet state, and the slow one is due to heat with the relaxation of triplet benzophenone. The solid line shows the curve best-fitted with a single-exponential equation.

experimentally obtain heat of reaction for the short-lived reaction intermediates such as AI tautomers.

Photothermal methods, *e.g.* TRTL and photoacoustic methods, are powerful techniques to study not only nonradiative but also radiative processes, and are exactly complementary to conventional optical methods.[20−25] Special care has to be exercised to obtain the absolute emission quantum yield by conventional optical methods: refractive index difference between sample and reference solutions, reabsorption, reemission, and polarization corrections.[26] Photothermal techniques can eliminate some of these experimental errors. The TRTL method enables us to instantaneously measure the heat released by nonradiative deactivation processes of photoexcited transient species such as excited singlets, triplets, isomers, and radicals, providing energetic and kinetic information with high sensitivity and accuracy of calorimetry.[20−25] In this paper, we applied the TRTL technique for the first time to the DPT reaction of AI dimer and complexes. The fluorescence quantum yields of dimer/complexes and its tautomers and the enthalpy change of the back DPT reaction were successfully obtained. We will discuss reaction dynamics of AI dimer and its complexes.

Experimental Section

TRTL experimental setup is described in Figure 2. An output of a dye laser (Molectron DL223; Rhodamine 640) pumped by a frequency-doubled Q-switched Nd^{3+}:YAG laser (Quantel Brilliant ω; 150 mJ/pulse at 532 nm, 5 ns pulse duration) was passed through a SHG crystal (KDP), and the frequency-doubled laser beam was used as an excitation light source for TRTL. The laser power attenuated through a variable neutral density filter (Corion 2161) was monitored with a silicon photodiode (Hamamatsu S1336-5BQ) calibrated with a pyroelectric detector (Gentec ED100) after part of the laser beam was introduced by a beam splitter. The sample solution was flowed in a cuvette (NSG T-59FL-10; 10 mm optical path length). A He−Ne laser beam (Uniphase 1103P; 2 mW) equipped with a stabilized power supply (Takasago; ARH500), used as an analyzing beam of TRTL signals, was focused in front of the sample cuvette with a 30 mm focal length lens collinerally to the excitation beam focused with a 150 mm flocal length lens. The He−Ne laser beam sampled through a pinhole (Corion 2401; 300 μm diameter) and a monochromator (Jasco CT-10; 0.5 nm resolution) was detected with a photomultiplier tube (Hamamatsu R928). The output signals were converted into the voltage with a 50 or 500 Ω load register, measured by a digital oscilloscope (Sony Tektronix TDS-380P; 2 GHz/Sampling), and transferred to a personal computer. The TRTL signals were normally averaged over 50 shots to improve the S/N ratio.

Transient absorption spectra were measured with the conventional laser flash photolysis system consisting of an excimer laser (Lumonics TE-860-4; XeCl, 308 nm, 10 ns) for an excitation light source and a steady-state Xe lamp (Ushio UXL-300DO; 300 W) for a monitoring light. In stepwise two-color laser excitation fluorescence measurements, the XeCl excimer laser was used as a photolysis light for the generation of tautomers, and the frequency-tripled YAG laser (355 nm) was as a probe laser to induce tautomer fluorescence. The arrival time of the probe laser to the photolysis laser was controlled by a handmade delay circuit. The two beams were introduced into the sample cell collinearly. The fluorescence was collected with a 80 mm focal length lens, and detected by the photomultiplier tube after passing through the monochromator with a glass filter (Toshiba cutoff filter Y45).

AI (Tokyo Kasei) was recrystallized from ethanol and dried under vacuum. The purity was checked with the fluorescence excitation spectrum.[8] Pyridazine (Tokyo Kasei) was purified by repeated trap-to-trap distillation under vacuum. Hexane, methanol, and acetic acid (Kanto Chemical Industry, GR grade) were used from freshly opened bottles. Samples were deaerated by bubbling Ar gas (purity 99.95%) purged by solvent vapors for half an hour before use, or were aerated in the 308 nm excitation to remove influence of triplet formation. All measurements were carried out at room temperature. Absorption spectra were measured with a double beam spectrophotometer (Jasco Ubest V-550). Fluorescence spectra corrected were obtained with a spectrofluorometer (Jasco FP-550A).

Results and Discussion

1. Quantum Yield of Triplet Formation (ϕ_{ISC}) for Benzophenone. First, to check our detection system, we carried out the TRTL measurement of benzophenone in benzene and determined the quantum yield of triplet formation. Figure 3 shows the typical TRTL signal of benzophenone in benzene with excitation by the 320 nm light. The lens signal is composed of the fast and slow rises and stays flat till *ca.* 1 ms. The fast component (U_F), which rises immediately after the laser irradiation, corresponds to the heat released through nonradiative deactivation processes from the initially excited singlet state to the first excited triplet state. The slow one (U_S), which exponentially grows, is due to the triplet benzophenone relaxing to the ground state and is analyzed with the least-squares fitting (Figure 3 solid line). The lifetime of the triplet benzophenone is determined to be 6.2 μs. The ϕ_{ISC} relates to the lens signal

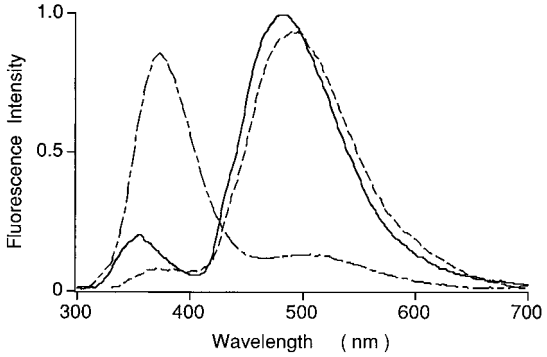

Figure 4. Fluorescence spectra of AI in hexane with (− − −) and without (—) acetic acid, and in methanol (− · −), excited with 320 nm steady light. Tautomer fluorescence appears mainly for the AI dimer and the AI−AcOH complex.

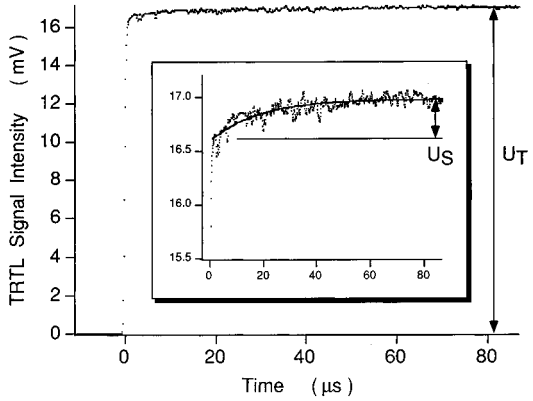

Figure 5. TRTL time profile of AI in hexane excited at 320 nm. The signal rises immediately and has a very small rising component as shown in the inset. The solid line is the curve best-fitted with a single-exponential equation. The rising time is determined to be 19 μs.

as follows:

$$\frac{U_S}{U_T} = \frac{\phi_{ISC} E_T}{E_{ex}} \tag{1}$$

Here, E_{ex} and E_T are energies of the excitation light (373 kJ/mol) and the triplet state for benzophenone (287 kJ/mol),[27] respectively, and U_T ($=U_F + U_S$) is called the total heat. The ϕ_{ISC} is determined to be 1.00 ± 0.01, which is identical to the reported value.[27]

2. Fluorescence Quantum Yields of Al Dimer/Complexes and Their Tautomers. Figure 4 shows emission spectra of AI in hexane with and without acetic acid (AcOH), and AI in methanol excited at 320 nm under the same experimental conditions. The light selectively excites the Al dimer and complexes, taking into account the association constants, K_a, and extinction coefficients.[3,14] Two bands appear in the violet and green visible regions. As reported previously, the former band is ascribed to excited dimer and/or complexes, and the latter is to its excited tautomer.[3,11] The tautomer fluorescence mainly appears in the AI dimer and AI−AcOH complex systems.

The TRTL signals of AI dimer in hexane were measured with the 320 nm irradiation. The time evolution of the TRTL signal was composed of almost fast (U_F) and of slightly slow (U_S) components shown in Figure 5. The fast component corresponds to the heat of the tautomer formation and the slow one to the heat released through the back DPT reaction. The slow rising component was analyzed with the single-exponential equation. The lifetime of tautomer in the ground state was determined to be 19 ± 2 μs, which was not affected by oxygen.

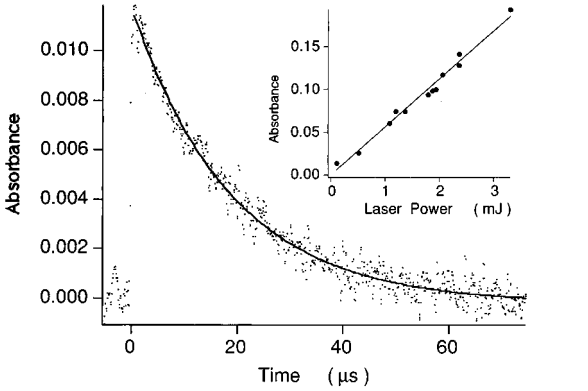

Figure 6. Transient absorption time profile monitored at 315 nm of AI in hexane excited at 308 nm, which decays in a single exponential. The solid line shows the best-fitting curve, and the lifetime of AI tautomer was determined to be 19 ± 1 μs. The laser power dependence of the transient absorption at $t = 0$ is shown in the inset.

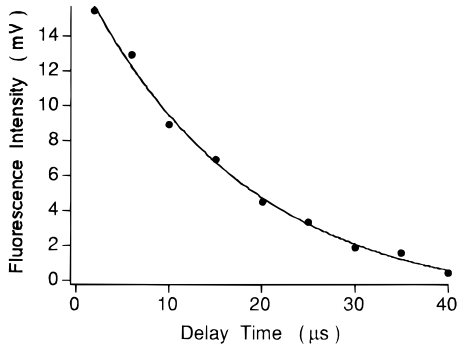

Figure 7. Fluorescence intensity of tautomer vs delay time between 308 and 355 nm laser beams. The tautomer, generated by the 308 nm excitation, was excited with the 355 nm laser. The decay was analyzed with least-squares fitting, and the tautomer lifetime was determined to be 17 ± 2 μs (solid line in the figure).

Figure 6 denotes transient absorption time profile monitored at 315 nm of AI in hexane excited at 308 nm, which decays in a single exponential. The solid line shows a best-fitting curve, and the lifetime of AI tautomer was determined to be 19 ± 1 μs, which is identical with the reported value.[12,13] The laser power dependence of the transient absorption at $t = 0$, shown in the inset of the figure, reveals the good linear relation. The fluorescence intensities of tautomer were plotted against the time interval between 308 and 355 nm laser beams in Figure 7. The tautomer, generated by the 308 nm excitation, was excited with the 355 nm laser. The decay was analyzed with the least-squares fitting, and the decay time was determined to be 17 ± 2 μs (solid line in the figure).

The lens signals at 90 μs after the laser excitation, when the reaction was completed, were plotted against the laser power in Figure 8 and show a good linear relation at each concentration of AI dimer. The slopes in Figure 8 are plotted against the absorptivity, $1-10^{-OD}$, in Figure 9. We determined the heat conversion efficiency, α, which is the fraction of the energy released as heat against the total energy absorbed. The α value was determined to be 0.90 ± 0.02 by comparing the slope in Figure 9 with that of pyridazine, which emits all the absorbed energy as heat.[22]

The fluorescence quantum yield (ϕ_f) is related with the α value as the equation of

$$\alpha = \frac{E_{ex} - \phi_f E_S}{E_{ex}} \tag{2}$$

where E_{ex} denotes excitation energy and E_S is 0−0 transition

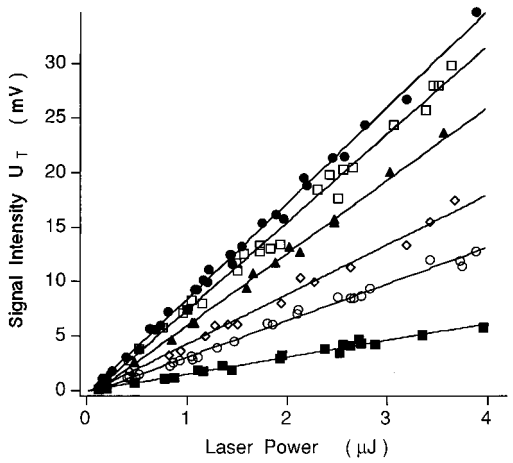

Figure 8. Laser power dependences of the total heat, U_T, at different concentrations of AI dimer. The solid lines are best-fitting curves obtained with the least-squares method. There are good linear relations between lens signal and laser power maintained in the range. Absorbances at 320 nm are 0.751 (●), 0.485 (□), 0.300 (▲), 0.195 (◇), and 0.090 (■).

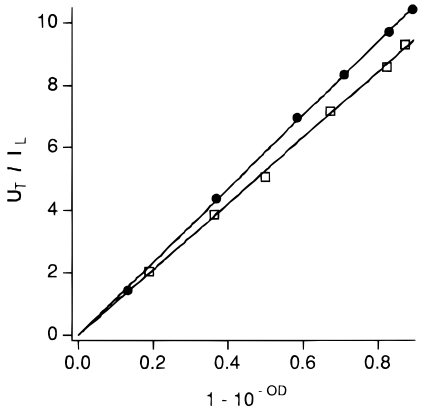

Figure 9. Plots of U_T/I_L against absorptivity, $1-10^{-OD}$, for AI dimer (□) and pyridazine (●). Data are fitted with the linear relation. The heat conversion efficiency, α, is obtained to be 0.90 ± 0.02 by comparison of the slopes.

energy. Consequently, the product $\Phi_f E_S$ is obtained from the evaluation of the α value. Since the fluorescence spectra usually spread over the wide energy range, we used the average energy, $\langle E_S \rangle$, instead of E_S. The $\langle E_S \rangle$ value is defined as

$$\langle E_S \rangle = \frac{\int I_f(\nu)\nu \, d\nu}{\int I_f(\nu) \, d\nu} \tag{3}$$

where $I_f(\nu)$ is the spectral distribution of fluorescence and ν is energy in wavenumbers. Since two types of fluorescence were observed in this system, eq 2 was rewritten as

$$\alpha = \frac{E_{ex} - \phi_f^N \langle E_S^N \rangle - \phi_f^T \langle E_S^T \rangle}{E_{ex}} \tag{4}$$

Here, superscripts of N and T show normal and tautomer, respectively. With the ratio of fluorescence intensity of ϕ_f^N/ϕ_f^T, which could be estimated from the fluorescence spectra, the fluorescence quantum yields of normal form, ϕ_f^N, and tautomer, ϕ_f^T, were successfully determined to be 0.16 and less than 0.01, respectively. These results including data on the complexes are summarized in Table 1. By comparing the fluorescence intensity with AI tautomer ($\phi_f^T = 0.16$), we can also estimate the fluorescence quantum yields of other complexes. The quantum yields estimated with fluorescence spectra for AcOH complex (0.12 for tautomer and 0.00_2 for normal fluorescence) are in good agreement with that obtained with TRTL (0.11 for tautomer and 0.00_2 for normal fluorescence). The total fluorescence quantum yield for methanol complex was 0.08. However, we could not obtain the value with the TRTL because the α value was over unity. This reveals there would be other reaction paths or rearrangement between AI and methanol molecules. The possibility of some other reaction is excluded because the absorption spectral change was not observed before and after several thousand laser shots. The reaction quantum yield was estimated to be less than 10^{-5}. It has been discussed that solvation should be important for the excited state dynamics of AI in protonated solvents.[6−11,14] Kim and Bernstein reported geometry and solvation shifted energy for AI dimer and its clusters with water and alcohols by time-of-flight mass spectroscopy.[17] The cluster binding energy is -1425 cm^{-1} for 1:1 AI/methanol and -2376 cm^{-1} for 1:2 clusters. Photoexcitation may produce macro size cluster from small complex in the methanol solution. Since the large cluster would be more stable, the α value will become larger than unity.

TABLE 1: Heat Conversion Efficiencies, α, Emission Quantum Yields, and Lifetimes of the AI Dimer, Its Complexes, and Their Tautomers

	k_r (μs)	$\langle E_S \rangle$ ($\times 10^4$ cm^{-1})	α	Φ_r TRTL	Φ_r fluor spectra[f]
AI dimer		2.77	0.90 ± 0.02	0.00_6	0.00_7
tautomer	19 ± 1,[a] 19,[d] 17[e]	1.92		0.16	0.16
	17 ± 2[b]				
	19 ± 2[c]				
AI−AcOH		2.66	0.94 ± 0.04	0.00_2	0.00_2
tautomer	*g*	1.88		0.11	0.12
AI−methanol	*g*	2.26	>1		0.08

[a] Determined with the transient absorption. [b] Determined with the two-color laser excitation. [c] Determined with the TRTL technique. [d] Reference 12. [e] Reference 13. [f] Obtained by comparing the fluorescence intensity with the AI tautomer. [g] Not detectable.

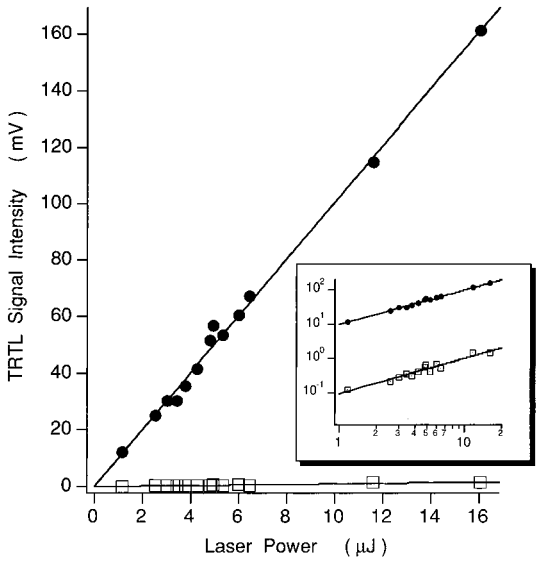

Figure 10. Plots of U_T/I_L and U_S vs laser power, I_L. Good linear relations are observed. The inset shows the log−log plots. The slopes in the inset, which were obtained with least-squares fitting, were determined to be 1.0 ± 0.1.

3. Determination of Reaction Enthalpy Change. Figure 10 shows the laser power dependence of U_T and U_S for the AI dimer. Good linear relations are observed. The slopes of the log−log plots (inset of Figure 10) were obtained to be 1.0 ±

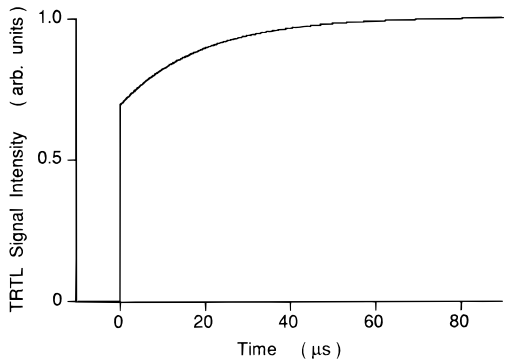

Figure 11. TRTL time profile simulated with the values of $\alpha = 0.90$, $\Phi_r = 1$, and $\Delta H = 102$ kJ/mol.

0.1. The slow component corresponds to the heat released with the back DPT reaction of the tautomer, and proportional to the quantum yield of the excited state DPT reaction, ϕ_r. The ratio of U_S/U_T is written as follows

$$\frac{U_S}{U_T} = \frac{\phi_r \Delta H}{\alpha E_{ex}} \tag{5}$$

where ΔH is the enthalpy change between dimer and tautomer in the ground state. The U_S/U_T value was obtained by comparing the slopes to be 0.012. The energy stored by the tautomer generation, $\phi_r \Delta H$, was determined to be 340 cm^{-1} with $E_{ex} = 31\,250$ cm^{-1} and $\alpha = 0.90$. The reaction quantum yield will be almost unity because of the following reasons. The quantum yield of normal fluorescence is quite low (0.00_6). The rate for the excited state DPT reaction was reported to be $>7 \times 10^{11}$ s^{-1} in the hydrocarbon solvents at room temperature.[5] Furthermore, there exist the two parallel reaction pathways to generate the AI dimeric tautomer.[5] The excited state DPT reaction of AI dimer occurred even from the zero vibrational level of the S_1 state and has no energy barrier.[16] Finally, the enthalpy change, ΔH, was estimated to be only 340 cm^{-1} (4 kJ/mol). This value is independent of the excitation wavelength.

It is surprising that the enthalpy change is quite low. Compared with other intramolecular proton transfer reaction, for example, the enthalpy change of keto-enol reaction for 7-hydroxyquinolinol in methanol was reported to be 41 kJ/mol.[21] For 2-methylbenzophenone, the reaction heat was obtained to be 116 kJ/mol for *cis*-enol and 202 kJ/mol for *trans*-enol.[25] The difference between the heat of formation of monomer AI and that of its tautomer was calculated to be 79 kJ/mol with *ab initio* calculation (6-31G).[28] As for the AI dimer and the dimeric tautomer, *ab initio* calculations were applied.[14,19,28] The results calculated are much higher than the value determined experimentally, that is, 94 kJ/mol (4-31G),[19] 102 kJ/mol (6-31G and 6-31G*).[14,28] Figure 11 denotes the simulation of TRTL time profile with the values of $\alpha = 0.90$, $\phi_r = 1$, and $\Delta H = 102$ kJ/mol. The slow rising feature is quite different from that in Figure 5. This will be explained with large conformational change from AI dimer to the tautomer or participation of the surrounding solvent molecules.

On the AcOH and methanol complexes, no slow rising component in TRTL signals was observed. Tokumura *et al.* reported that the transient absorption spectra of monomeric tautomer are identical to that of dimeric tautomer;[13] however, we could not find any transient absorption in the complex systems. Tautomer fluorescence was not detected with the stepwise two-color laser excitation as observed in the AI dimer system. Therefore, the back DPT reactions of complex tautomers probably proceed within the time resolution of our detection system (<100 ns). It was reported that the DPT reaction in AI dimer is promoted by the intermolecular stretching vibrational mode.[16] Sato and Iwata proposed a two-dimensional model and numerically solved the Schrödinger equation to show how the intermolecular vibration promotes the reaction.[29] The short lifetime of the complex tautomer in the ground state would result from the intermolecular low-frequency vibrational mode between AI and solvent molecules in the complex.

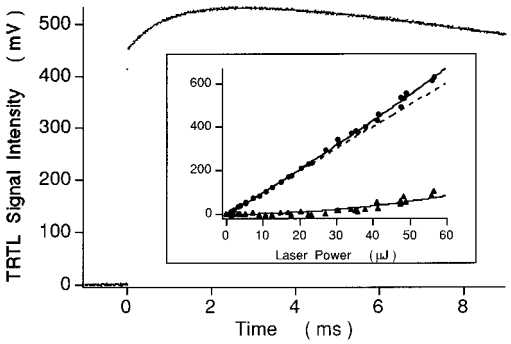

Figure 12. TRTL time profile of AI dimer excited at 320 nm under the high photon density region (48 μJ). The signal is composed of the steep rise and rather slow rise, and decays by the thermal diffusion. The slow component, depending on second order of laser power, is due to the heat released with the recombination of monomeric tautomer, which is generated by the two-photon absorption. The inset shows the laser power dependence in the high photon density region. The solid line was obtained with the least-squares fitting of the equation $U = aI_L + bI_L^2$. The dotted line is the fitting curve obtained with the linear equation in the low laser power region.

4. Reaction under Multiphoton Excitation of the AI Dimer. TRTL signals were measured under the high photon density region, shown in Figure 12. A rather slow rising component was observed, and the signal decays due to thermal diffusion. The laser power dependence at 3 ms after the laser excitation, shown in the inset of Figure 11, is curved in the range larger than 20 μJ, and well-fitted with the equation of $U = aI_L + bI_L^2$. Especially, the slow component, U'_s, mainly shows two-photon dependence remarkably. Under the high photon density condition, the long-lived species was reported to be monomeric tautomer.[13] It is concluded that the excited dimeric tautomer, generated by two-photon absorption, probably dissociates into the monomeric tautomer, which recombines within *ca.* 2 ms. As a result, reaction heat, which depends on the second order of photon density, should be released.

Conclusion

We successfully applied the TRTL technique to the determination of quantum yields for the normal and tautomer fluorescence and the enthalpy differences for tautomer formation by excitation of AI dimer and its complexes with AcOH and methanol. The quantum yields of normal fluorescence were determined to be less than 0.01, and those of tautomer fluorescence were 0.16 for the AI dimer and 0.11 for the AI-AcOH complex. The enthalpy change (340 cm^{-1}) between the AI dimer and its tautomer in the ground states was found to be very much lower than that estimated with *ab initio* calculations. It is suggested that the large conformational change between the normal and tautomer forms and/or the solvation effect of the surrounding molecule would play an important role. The fact that the heat conversion efficiency is larger than unity in the AI−methanol complex is also realized with the solvation effect, which would be responsible for a larger cluster formation. The TRTL results under the high photon density reveal that the AI dimer easily absorbs a second photon to dissociate into two monomeric tautomers followed by recombination in *ca.* 2

ms with reaction heat, which depends on the second order of photon density.

Acknowledgment. We thank Professor K. Fuke (Kobe University) for giving us the opportunity for this research. We also thank Professor S. Iwata (IMS) and Dr. K. Watanabe (Keio University) for providing the results of their calculations prior to publication. The present research was supported in part by a Grant-in-aid for Encouragement of Young Scientists (No. 08740449) and a Grant-in-aid for Scientific Research on Priority Area "Photoreaction Dynamics" (No. 06239103) from the Ministry of Education, Science, Sports and Culture, Japan.

References and Notes

(1) Taylor, C. A.; El-Bayoumi, M. A.; Kasha, M. *Proc. Natl. Acad. Sci. U.S.A.* **1969**, *63*, 253.
(2) Ingham, K. C.; Abu-Elgheit, M.; El-Bayoumi, M. A. *J. Am. Chem. Soc.* **1971**, *93*, 5023.
(3) Ingham, K. C.; El-Bayoumi, M. A. *J. Am. Chem. Soc.* **1974**, *96*, 1674.
(4) Hetherington, W. M., III; Micheels, R. H.; Eisenthal, K. B. *Chem. Phys. Lett.* **1979**, *66*, 230.
(5) Share, P.; Pereira, M.; Sarisky, M.; Repinec, S.; Hochstrasser, R. M. *J. Lumin.* **1991**, *48/49*, 204.
(6) Moog, R. S.; Maroncelli, M. *J. Phys. Chem.* **1991**, *95*, 10359.
(7) Chou, P.; Martinez, M. L.; Cooper, W. C.; McMorrow, D.; Collin, S. T.; Kasha, M. *J. Phys. Chem.* **1992**, *96*, 5203.
(8) Chen, Y.; Rich, R. L.; Gai, F.; Petrich, J. W. *J. Phys. Chem*. **1993**, *97*, 1770.
(9) Chen, Y.; Gai, F.; Petrich, J. W. *J. Am Chem. Soc.* **1993**, *115*, 10158.
(10) Chen, Y.; Gai, F.; Petrich, J. W. *J. Chem. Phys. Lett*. **1994**, *222*, 329.
(11) Chang, C.; Wen-Chi, H.; Meng-Shin, K.; Chou, P.; Clements, J. H. *J. Phys. Chem.* **1994**, *98*, 8801.
(12) Tokumura, K.; Watanabe, Y.; Itoh, M. *J. Phys. Chem*. **1986**, *90*, 2362.
(13) Tokumura, K.; Watanabe, Y.; Udagawa, M.; Itoh, M. *J. Am. Chem. Soc.* **1987**, *109*, 1346.
(14) Chou, P.; Wei, C.; Chang, C.; Meng-Shin, K. *J. Phys. Chem.* **1995**, *99*, 11994.
(15) Fuke, K.; Yoshiuchi, H.; Kaya, K. *J. Phys. Chem.* **1984**, *88*, 5840.
(16) Fuke, K.; Kaya, K. *J. Phys. Chem.* **1989**, *93*, 614.
(17) Kim, S. K.; Bernstein, E. R. *J. Phys. Chem.* **1990**, *94*, 3531.
(18) Douhal, A.; Kim, S. K.; Zewail, A. H. *Nature* **1995**, *378*, 260.
(19) Douhal, A.; Guallar, V.; Moreno, M.; Lluch, J. M. *Chem. Phys. Lett*. **1996**, *256*, 370.
(20) Braslavsky, S. E.; Heibel, G. E. *Chem. Rev.* **1992**, *92*, 1381.
(21) Terazima, M.; Azumi, T. *J. Am. Chem. Soc.* **1989**, *111*, 3824.
(22) Suzuki, T.; Kajii, Y.; Shibuya, K.; Obi, K. *Res. Chem. Intermed.* **1991**, *15*, 261.
(23) Suzuki, T.; Kajii, Y.; Shibuya, K.; Obi, K. *Chem. Phys.* **1992**, *161*, 447.
(24) Suzuki, T.; Kajii, Y.; Shibuya, K.; Obi, K. *Bull. Chem. Soc. Jpn.* **1992**, *65*, 1084.
(25) Suzuki, T.; Okuyama, U.; Ichimura, T. *Chem. Phys. Lett.* **1997**, *266*, 107.
(26) Demas, J. N.; Crosby, G. A. *J. Phys. Chem.* **1971**, *75*, 991.
(27) Murov, S. L.; Carmichael, I.; Hug, G. L. *Handbook of Photochemistry*, 2nd ed.; Marcel Dekker: New York, 1993.
(28) Watanabe, H.; Iwata, S., private communication.
(29) Sato, N.; Iwata, S. *J. Chem. Phys.* **1988**, *89*, 2932.